Compact Modelling of Chirality and Contact Resistance Effects in CNTFETs

Achsah Gladith N[1*], *T. J. Nagalakshmi*[1]

[1]Saveetha School of Engineering, SIMATS Engineering, Saveetha Institute of Medical and Technical Sciences, Saveetha University, Chennai, Tamil Nadu, India.

Abstract. This work presents a compact, semi-empirical modelling framework for Carbon Nanotube Field-Effect Transistors (CNTFETs) based on the impact of chiralitydependent electronic properties and contact resistance. The diameters and bandgaps of (10,0), (8,3), and (7,5) CNTs are computed from lattice geometry. The drain current is modelled using a subthreshold formulation coupled with a velocity saturation function. The internal drain bias is solved self-consistently to incorporate series contact resistance. Transfer characteristics and Output characteristics are simulated for all three chiralities, which are used to extract the ON current, OFF current, ON/OFF ratio, and peak transconductance values. Results show that increasing contact resistance significantly reduces the effective channel bias, suppressing ON-state conduction and degrading overall energy performance. The paper provides a computationally efficient approach for evaluating chirality-specific CNTFET behaviour and quantifying the impact of contact engineering on nanoscale device operation.

Keywords:CNTFET, Energy, Chirality, Contact resistance, Performance, Characteristics, Bandgap.

1 Introduction

Device performance of transistors is increasingly constrained by short channel effects, parasitic resistances and rising power density, as silicon CMOS technology approaches its physical and scaling limits below the 5 nm regime. These limitations have intensified the search for alternative channel materials capable of sustaining high drive current, strong electrostatic control and improved energy efficiency [1][2]. Single WalledCarbon nanotube field effect transistors (SW-CNTFETs) have emerged as one of the most promising candidates for next generation nanoelectronics due to their quasi 1D structure, high carrier mobility and excellent gate coupling[3]. Recent studies highlight that CNTFETs can surpass silicon MOSFETs in ON current, switching efficiency, and energy delay product, making them strong contenders for post silicon logic technologies [4].

* Corresponding author:nagalakshmitj.sse@saveetha.com

Chirality plays a central role in determining CNT electronic properties, as the (n, m) indices directly define the nanotube diameter and bandgap, thereby influencing threshold voltage and current drive [5]. Advances in chirality engineering have enabled more predictable control of CNT electronic behaviour to support the development of high performance and low power CNT based devices [6]. Furthermore, wafer scale methods for producing ordered CNT architectures have improved material uniformity and device reproducibility, strengthening the feasibility of CNT based integrated systems [7].Despite these advantages, contact resistance remains a major bottleneck in CNTFET performance. Studies show that in aggressively scaled devices, parasitic contact resistance can significantly limit current injection, degrade transconductance and reduce switching efficiency [8]. Continued progress in contact engineering through optimized doping, interface design and metal-CNT coupling is therefore essential for realizing the full potential of CNTFETs in practical circuits [9]. Carefully engineered contacts can achieve low n-type resistance values even at nanoscale contact lengths, underscoring the importance of interface optimization.

Simulation frameworks based on quantum transport and compact modelling have become indispensable for understanding CNTFET behaviour and guiding device design [10]. Modern computational studies explore switching limits, tunnelling effects and electrostatic control in CNTFETs [11]. This provides insights into their performance under realistic operating conditions [12]. These modelling efforts complement experimental advances and support the development of CNTFET [13] based digital circuits including SRAM cells and logic blocks, demonstrating their applicability in low power nano electronic systems [10][11]. The paper investigates the impact of chirality dependent bandgap variation and contact resistance on CNTFET electrical characteristics. By analysing transfer and output behaviour across multiple chiralities and resistance values using MATLAB, the intrinsic and extrinsic factors governing CNTFET performance are analysed.

2 Methodology

This work evaluates the electrical behaviour of CNTFETs based on intrinsic nanotube chirality and extrinsic contact resistance. Three semiconducting chiralities (10,0), (8,3), and (7,5) are each characterized by its diameter dependent bandgap and threshold voltage. A compact, physics based current model is used to simulate transfer and output characteristics under varying gate and drain biases.Performance is compared across chiralities and across varying contact resistance values to provide a systematic assessment of their impact on current drive, switching ratio, and transconductance. The electrical behaviour of a carbon nanotube is strongly determined by its chirality (n, m), which sets the tube diameter and bandgap. For each selected chirality (10,0), (8,3), (7,5), the CNT diameter is computed [12] using equation (1).

$$D_{\mathrm{CNT}} = \frac{\sqrt{3}\,b}{\pi}\sqrt{n^2 + m^2 + nm} \tag{1}$$

where b=1.44nm is the C–C bond length. The electronic bandgap follows the inverse diameter relation given by equation(2),

$$E_g = \frac{2a|E_\pi|}{D_{\mathrm{CNT}}} \tag{2}$$

Here, $a = \sqrt{3}\,b$ and Eπ = -2.7 eV. The threshold voltage is approximated from the mid gap position shown in equation (3).

$$V_T = \frac{E_g}{2} \tag{3}$$

This is in consideration of the device physics between chirality, diameter, bandgap, and device ON/OFF behaviour. The simulation assumes a coaxial-gate CNTFET

architecture, which provides symmetric electrostatic control around the nanotube.The model assumes quasi-ballistic transport, which is appropriate for short-channel CNTFETs where the mean free path is comparable to the channel length. Scattering mechanisms are not explicitly included, and therefore the ON currents that are simulated represents an upper-bound estimate. This geometry is consistent with the transport equations employed in this work.

The simulations were performed at room temperature (300 K). Temperature influences thermal voltage and phonon-limited mobility, but the comparative behaviour across chiralities and contact-resistance values remains unchanged under this assumption.A semi-empirical compact model is used to capture the essential transport behaviour of a CNTFET while remaining computationally efficient [13].

The drain current is expressed in equation (4)as,

$$I_D = I_0 ln\left(1 + \exp\left(\frac{V_{GS}-V_T}{V_{\text{th,eff}}}\right)\right).f(V_{DS,\text{int}}) \quad (4)$$

where I_0 sets the current scale and $V_{th,eff}$smooths the subthreshold transition. The drain voltage dependent function is modelled in equation (5) as,

$$f(V_{DS,\text{int}}) = \frac{V_{DS,\text{int}}}{V_{DS,\text{int}}+V_{\text{sat}}} \quad (5)$$

Represents velocity saturation in a 1D channel. To incorporate contact resistance, the internal drain voltage is solved self-consistently using equation (6),

$$V_{DS,\text{int}} = V_{DS} - I_D R_C \quad (6)$$

This captures the reduction in effective bias across the channel due to series resistance at the metal-CNT interface. Ambipolar conduction is suppressed in this model by assuming a sufficiently large Schottky barrier for hole injection at the drain contact. This reflects a unipolar n-type CNTFET configuration and is consistent with the focus on electrondominated transport.

For each chirality, the standard device characteristics are evaluated based on transfer characteristics plot and output characteristics plot [14]. From the simulated characteristics, derived parameters such as ON current, OFF current, ON/OFF ratio and peak transconductance (g_m) are calculated. A separate sweep is performed for the (10,0) CNT to analyse the effect of contact resistance with the set of contact resistances, $R_C \in$ {0, 10kΩ, 50kΩ, 100kΩ}. The derived parameters are calculated for each varying contact resistance value. This gives an overview on the impact of contact resistance on CNTFET.As the focus is on current conduction and contact-resistance effects, quantum and gate-oxide capacitances are not included in this compact model. While this omission affects charge-based metrics such as delay and subthreshold slope, it does not impact the comparative trends in ON current and transconductance presented in this work.

3 Results

The CNTFETs based on chiralities (10,0), (8,3), and (7,5) were characterised using MATLAB and are analysed to capture the impact of diameter on threshold voltage, ON current, and output characteristics. Across all CNTFET devices, increasing gate bias enhances channel conduction, while higher drain bias increases current saturation. A separate analysis of contact resistance shows a strong degradation in ON current, ON/OFF ratio, and transconductance values as $R_C$increases.This confirms that metal-CNT interface resistance is a dominant performance limiter in CNTFETs.

3.1 Transfer Characteristics

The Transfer characteristics graph of (10,0) CNTFET in Fig.1 shows a strong and smooth increase in drain current with increase in gate voltage which reflects its relatively small bandgap and low threshold voltage. Higher drain biases produce noticeably larger currents which indicates efficient carrier injection and strong gate control across the operating range.

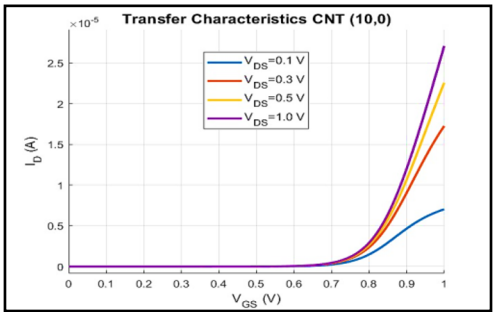

Fig. 1. Transfer Characteristics of CNTFET, CNT - (10,0).

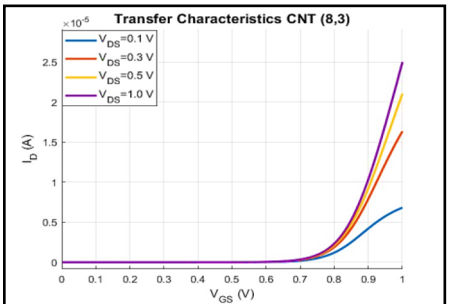

Fig. 2. Transfer Characteristics of CNTFET, CNT - (8,3).

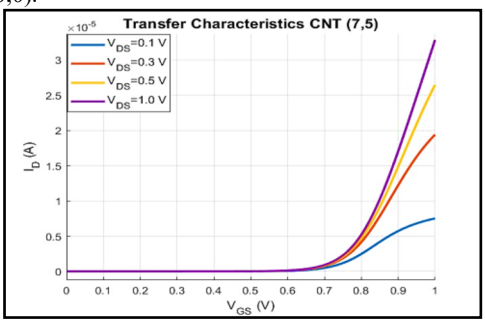

Fig. 3. Transfer Characteristics of CNTFET, CNT - (7,5).

In the transfer characteristics graph of (8,3) CNTFET shown in Fig.2, the drain current rises steadily with gate voltage but with lower magnitude compared to the (10,0) CNT due to its larger bandgap. The separation between curves at different drain biases remains clear which shows consistent modulation of channel conduction with both gate and drain voltages.

The transfer characteristics of (7,5) CNTFET in Fig.3, exhibits the weakest conduction among the three chiralities, consistent with its higher bandgap and increased threshold voltage. Current increases with gate voltage for all drain biases. But the overall levels remain lower, highlighting the stronger bandgap limited transport due to narrower diameter of the nanotube.

The transfer characteristics for all three chiralities show a monotonic rise in drain current with increasing gate voltage, with the curves shifting rightward as the bandgap increases. Higher drain bias produces higher current levels, due to enhanced channel drive. The (10,0) CNT, having the largest diameter among the three CNTFETs, shows the smallest bandgap and therefore the earliest turn on and highest ON current. In contrast, the (7,5) CNThas smallest diameter,and exhibits a larger bandgap and correspondingly reduced conduction. The (10,0) device displays the strongest conduction, while the (7,5) device

shows the weakest, which illustrates the impact of chirality dependent bandgap on threshold voltage and current drive.

3.2 Output Characteristics

The output characteristics graph of (10,0) CNTFET in Fig.4 exhibits strong output conduction, with the drain current rising rapidly at low V_{DS} and gradually approaching saturation as the drain bias increases. Higher gate voltages produce significantly larger currents, reflecting efficient carrier injection and the relatively small bandgap of this chirality. The device shows clear and well defined linear and saturation regions across all gate biases.

The output characteristics of (8,3) CNTFET seen in Fig.5, shows that the drain current increases steadily with V_{DS}, but the overall current levels are lower than those of the (10,0) device due to its larger bandgap. The curves maintain distinct separation for different gate voltages, indicating consistent gate control. Saturation behaviour is present but less pronounced, reflecting the reduced drive capability of this nanotube.

The (7,5) CNTFET in Fig.6, shows the weakest output current among the three chiralities, consistent with its higher bandgap and increased threshold voltage. Current rises with both drain and gate bias, but the magnitude remains comparatively low and saturation occur at reduced levels. The device demonstrates clear gate dependent modulation despite its more limited conduction.

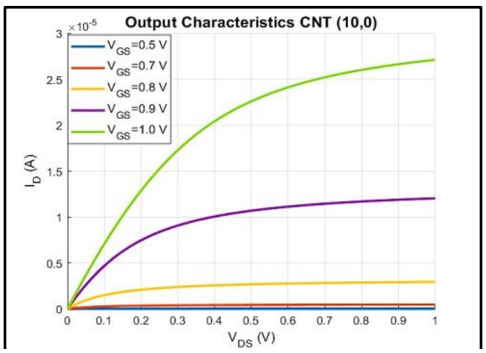

Fig. 4. Output Characteristics of CNTFET, CNT - (10,0).

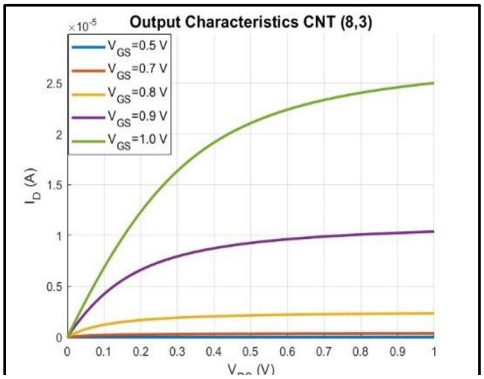

Fig. 5. Output Characteristics of CNTFET, CNT - (8,3).

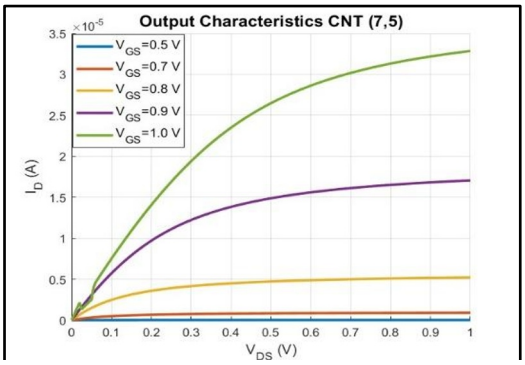

Fig. 6. Output Characteristics of CNTFET, CNT - (7,5).

The observed overall output characteristics shows that each device exhibits a clear linear region at low drain bias followed by gradual saturation, as the channel approaches velocity saturation. CNTs with larger diameters produce higher saturation currents, and the separation between curves at different gate voltages becomes more pronounced for chiralities with smaller bandgaps. The (10,0) CNT therefore shows the highest output current, followed by (8,3) and (7,5), consistent with their respective bandgaps.

The performance summary tabulated in Table. I compare CNTFETs with (10,0), (8,3), and (7,5) chiralities, highlighting the influence of diameter dependent bandgap variations on device behaviour. The (10,0) and (8,3) nanotubes show similar diameters and bandgaps resulting in comparable threshold voltages and ON currents.The slightly wider (7,5) tube exhibits a lower bandgap and correspondingly higher conduction.

Table I. Performance summary of CNTFETs at (10,0), (8,3) and (7,5) chiralities.

Parameters	**(10,0)**	**(8,3)**	**(7,5)**
Diameter, (nm)	0.794	0.782	0.829
Bandgap, (eV)	1.696	1.722	1.625
Threshold voltage, (V)	0.848	0.861	0.812
I_{ON}, (A)	2.711 e-5	2.502 e-5	3.285 e-5
I_{OFF}, (A)	3.899 e-13	3.005 e-13	7.974 e-13
I_{ON}/I_{OFF}	6.951 e+7	8.324 e+7	4.119 e+7
G_m(max), (S)	1.605 e-4	1.596 e-4	1.608 e-4
G_{ds}(sat), (S)	4.317 e-6	3.799 e-6	5.997 e-6

OFF currents remain in the sub picoampere range for all devices, leading to ON/OFF current ratios on the order of 10^7. The maximum transconductance values are nearly identical across chiralities indicating similar gate coupling efficiency. The output conductance in saturation shows modest variation, reflecting differences in output resistance linked to chirality dependent transport.

4 Discussion

Recent studies indicate that contact resistance remains a dominant extrinsic factor limiting CNTFET performance, particularly as devices scale toward shorter channel lengths and higher integration densities [14][15]. The metal-CNT interface critically governs carrier injection efficiency, effective carrier mobility, and the achievable ON-state current. Consequently, accurate modelling of contact resistance is essential for realistic evaluation and predictive simulation of CNTFET behaviour.

Table II. Performance Metrics based on varying Contact resistance.

R_C (KΩ)	**I_{ON} (A)**	**I_{OFF} (A)**	**I_{ON}/I_{OFF}**	**G_m(max) (S)**
0	2.802 e-5	3.899 e-13	7.186 e+7	1.731 e-4
10	2.710 e-5	3.899 e-13	6.951 e+7	1.605 e-4
50	1.742 e-5	3.899 e-13	4.468 e+7	9.973 e-5
100	7.411 e-6	3.899 e-13	1.901 e+7	1.056 e-4

Table II summarizes the increase in contact resistance that progressively degrades CNTFET performance. As RC rises from 0 to 100 KΩ, ON current keeps decreasing, but OFF current remains unchanged reflecting its weak dependence on series resistance. This leads to a steady reduction in the ON/OFF ratio, indicating diminished switching capability at higher contact resistance. The maximum transconductance also declines with increasing R_C showing reduced gate driven modulation of channel charge. Overall, the data highlights the strong sensitivity of CNTFET performance to contact resistance at the metal-nanotube interface.

The two plots in Fig.7 illustratesthe key performance metrics of the CNTFET with increasing contact resistance. The ON/OFF ratio decreases steadily as R_C increases from 0 to 100 KΩ, reflecting the reduction in ON state current while the OFF current remains essentially unchanged. The transconductance curve shows a similar sensitivity, with g_m(max) dropping sharply at lower resistance values and then varying more gradually at higher R_C. Together, the graphs highlight the progressive loss of switching efficiency and gate driven modulation as contact resistance becomes more significant

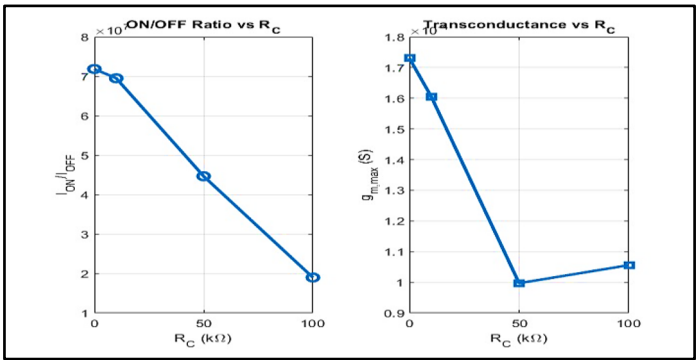

Fig. 7. Contact Resistance (R_C) Vs ON/OFF ratio and Transconductance for (10,0) CNTFET.

5 Conclusion

This paper uses a compact, physics-based modelling approach to examine the electrical behaviour of CNTFETs based on chirality and contact resistance. The analysis of the three chiralities shows clear differences in threshold voltage and current drive, with larger diameter nanotubes exhibiting stronger conduction due to their smaller bandgaps. The output and transfer characteristics consistently reflected these intrinsic material properties. The contact resistance analysis demonstrated that increasing contact resistance significantly reduces ON current, ON/OFF ratio, and transconductance, while leaving the OFF current largely unaffected. These results highlight the combined importance of chirality selection and interface engineering in determining CNTFET performance. Overall, the findings reinforce that both intrinsic nanotube geometry and extrinsic contact quality play decisive roles in enabling high efficiency nanoscale transistor operation.

References

1. R. Rajasekhar, B. Yakkala, Comparison of VI characteristics between MOSFET and BIOFET by varying materials, ECS Trans. 107, 1, 12595 (2022), https://doi.org/10.1149/10701.12595ecst

2. B. Nagappan, K. Mehar, S.P. Prashanth, D.R. Vaghela, S. Samantaray, C.P. Sahu, A. Smerat, K.K. Priya, Advanced functionalization strategies of diamond and diamond-like carbon for emerging applications in sensing, electronics, and energy conversion, Carbon Trends (2025), 100584, https://doi.org/10.1016/j.cartre.2025.100584
3. L. Natrayan, S. Angalaeswari, S. Kaliappan, C.N.D.K. Reddy, V. Sivaprakash, P.P. Patil, P. Murugan, Reduction of 1/f noise in single-walled carbon nanotubes (SWCNTs) using gas adsorption technique, Adsorpt. Sci. Technol. 2022, 3244702 (2022), https://doi.org/10.1155/2022/3244702
4. Z. Zhang, N. Zhang, Z. Zhang, High performance carbon nanotube electronic devices: Progress and challenges, Micromachines (Basel) 16, 554 (2025), https://doi.org/10.3390/mi16050554
5. J. Doumani, M. Lou, O. Dewey, N. Hong, J. Fan, A. Baydin, et al., Engineering chirality at wafer scale with ordered carbon nanotube architectures, Nat. Commun. 14, 7380 (2023), https://doi.org/10.1038/s41467-023-43199-x
6. S. Sen, A. Sarkar, P. Chakraborty, Characterization and investigating the effect of gate-insulator thickness on co-axial cylindrical carbon nanotube field effect transistor, Adv. Sci. Technol. Eng. Syst. J. 8, 12–16 (2023), https://dx.doi.org/10.25046/aj080102
7. S. Hu, K. Luo, H. Zhao, Y. Xie, X. Fu, Charge transport in carbon nanotube field-effect transistors: foundations for carbon-based nanoelectronics, Moore and More 3, 1, 2 (2026), https://doi.org/10.1007/s44275-026-00042-x
8. G. Fan, K.L. Low, Physics-integrated machine learning for efficient design and optimization of a nanoscale carbon nanotube field-effect transistor, ECS J. Solid State Sci. Technol. 12, 9, 091005 (2023), https://doi.org/10.1149/2162-8777/acfb38
9. A. Sanchez-Soares, C. Gilardi, Q. Lin, T. Kelly, S.-K. Su, G. Fagas, et al., Switching limits of top-gated carbon nanotube field-effect transistors, Solid-State Electron. 202, 108624 (2023), https://doi.org/10.1016/j.sse.2023.108624
10. E. Jolly, V.K. Sharma, A.K. Bhardwaj, Comprehensive analysis of CNTFET-based low-power SRAM cell, Analog Integr. Circuits Signal Process. 126, 3, 46 (2026), https://doi.org/10.1007/s10470-026-02577-3
11. S.U. Haq, E. Abbasian, T. Khurshid, et al., Overcoming silicon MOSFET limitations with chirality-engineered CNTFETs: a ternary half adder demonstration for next-generation nanoelectronics, Silicon 18, 249–264 (2026), https://doi.org/10.1007/s12633-025-03551-w
12. W. Huang, L. Chen, A compact model of carbon nanotube field-effect transistors for various sizes with bipolar characteristics, Electronics 13, 1355 (2024),https://doi.org/10.3390/electronics13071355
13. Y. Zhang, X. Li, M. Wang, J. Liu, H. Zhao, Novel extraction method for contact resistance and effective mobility in carbon nanotube field-effect transistors using S-parameter measurements, Results Phys. 53, 106999 (2023),https://doi.org/10.1016/j.rinp.2023.106999
14. H.-Y. Chiu, Y.-C. Chen, C.-H. Lin, S.-K. Su, M. Passlack, Self-aligned contact doping for performance enhancement of low-leakage carbon nanotube field effect transistors, Adv. Electron. Mater. 10, 2300519 (2024), https://doi.org/10.1002/aelm.202300519
15. H.-Y. Huang, Y.-C. Chen, C.-H. Lin, S.-K. Su, Improving contact resistance in top-gate carbon nanotube transistor through Self-Aligned MoO xnanoparticle contact doping, ACS Appl. Electron. Mater.8, 256–264 (2025),https://doi.org/10.1109/TED.2024.3423748